Nonlinear oscillations of coalescing magnetic flux ropes

Dmitrii Y. Kolotkov,[*] Valery M. Nakariakov,[†] and George Rowlands
Centre for Fusion, Space and Astrophysics, Department of Physics, University of Warwick, CV4 7AL, United Kingdom

An analytical model of highly nonlinear oscillations occurring during a coalescence of two magnetic flux ropes, based upon two-fluid hydrodynamics, is developed. The model accounts for the effect of electric charge separation, and describes perpendicular oscillations of the current sheet formed by the coalescence. The oscillation period is determined by the current sheet thickness, the plasma parameter β, and the oscillation amplitude. The oscillation periods are typically greater or about the ion plasma oscillation period. In the nonlinear regime, the oscillations of the ion and electron concentrations have a shape of a narrow symmetric spikes.

I. INTRODUCTION

A current sheet is one of the fundamental building blocks of natural and laboratory plasma systems, e.g., [1,2]. An important phenomenon is a coalescence of two magnetic islands, which occurs in the interaction of two twisted magnetic flux tubes (ropes) of the same sign of helicity. This process is believed to occur in very different plasma environments, for instance, the solar corona, e.g., [3,4], Earth's magnetosphere, e.g., [4,5], magnetar atmospheres, e.g., [6], and laboratory plasmas, e.g., [7]. Dynamical processes in current sheets have interesting observational manifestations, in particular various oscillations detected remotely and *in situ*, e.g., [8–11]. An analytical two-fluid model of the nonlinear stage of the coalescence process, designed by [12] predicts a highly nonlinear oscillatory regime.

In the model of [12] (Fig. 1) two co-aligned plasma currents j_z generate poloidal magnetic fields which are oppositely directed along the y axis in the region of the coalescence, which thus becomes a current sheet. It was numerically found that in the explosive regime of the coalescence there appears a specific spatial scale λ of the poloidal magnetic field (small in comparison with the radii of the colliding magnetic ropes R), where the field lines can be considered as straight, and the current sheet can be considered as one-dimensional. Hence for transverse oscillations of the current sheet, one can take that $\partial/\partial x \gg \partial/\partial y, \partial/\partial z$ and $\nabla = \{\partial/\partial x, 0, 0\}$. The oscillation could be described by perturbations of the electric field $\mathbf{E} = \{E_x, 0, E_z\}$ and magnetic field $\mathbf{B} = \{0, B_y, 0\}$, the bulk plasma velocities of ion and electron plasma species $\mathbf{V}_{i,e} = \{V_{x\,i,e}, 0, V_{z\,i,e}\}$, and the variations of the ion n_i and electron n_e concentrations. In this definition of the electric field $\mathbf{E}$, the x component E_x is related to the electrostatic field generated by the electric charge separation according to Poisson's law, while the z component E_z is the induced electric field by Faraday's law. Dynamics of these quantities is govern by two-fluid hydrodynamic equations and Maxwell equations.

In [12] self-similar solutions of the governing equations were obtained by introducing dimensionless time-dependent scale factors $a = a(t)$ and $b = b(t)$ separately for electron and ion dynamics, respectively, connected with the plasma species concentrations as $n_e = n_0/a$, and $n_i = n_0/b$, where $n_0 = n_e = n_i$ is the equilibrium concentration. Authors of [12] obtained an analytical solution of the problem only for the limiting case when $a = b$, and, hence, the electron and ion plasma concentrations were taken to be strictly equal to each other, $n_e = n_i$. The electrostatic field E_x was considered to be nonzero, which is a crucial condition for the oscillatory behavior of the current sheet, generated by this mechanism. Strictly speaking, this so-called quasineutrality assumption is valid only for low-frequency processes. However, the model contains the nonzero value of the electron mass m_e, as well as the finite values of the electron and ion plasma frequencies ω_e and ω_i. Hence, it would be natural to expect that the model also describes high-frequency oscillations, where the electric charge separation effects are important.

In this letter we demonstrate the possibility of a nonlinear oscillatory regime of the evolution of a current sheet formed by a coalescence of two magnetic ropes. The scale factors $a(t)$ and $b(t)$ are considered to be not equal to each other, i.e., the local electric charge separation is allowed. Our solution covers both low-frequency oscillations, including the limiting case $n_e = n_i$, considered in [12], and the high-frequency case where the electric charge separation cannot be neglected.

II. ANALYSIS

Under the simplifying assumptions described above, it was shown in [12] that the evolution of a current sheet is governed by the following equations [namely, Eqs. (23) and (24) in [12]]:

$$\frac{d^2 a}{d t^2} = -\omega_e^2 \left(\frac{a}{b} - 1\right) - \frac{m_i}{m_e} \frac{V_A^2}{\lambda^2 a^2} + \frac{m_i}{m_e} \frac{V_s^2}{\lambda^2 a^\gamma}, \quad (1)$$

$$\frac{d^2 b}{d t^2} = \omega_i^2 \left(1 - \frac{b}{a}\right), \quad (2)$$

where $\omega_{e,i}^2 = 4\pi n_0 e^2/m_{e,i}$ are electron and ion plasma frequencies; $V_A^2 = B_0^2/4\pi m_i n_0$ is the Alfvén speed, with B_0 and n_0 being the equilibrium values of the poloidal magnetic field and plasma concentration; $V_s^2 = P_0/m_i n_0$ is sound speed, with P_0 being the equilibrium thermodynamic gas pressure; γ is

_____
[*]D.Kolotkov@warwick.ac.uk
[†]Also at School of Space Research, Kyung Hee University, Yongin, 446-701, Gyeonggi, Korea, and Central Astronomical Observatory at Pulkovo of the Russian Academy of Sciences, St Petersburg 196140, Russia.
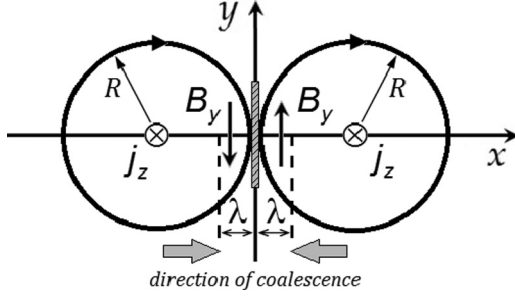
FIG. 1. Formation of a thin 1.5D current sheet (the hatched vertical slab) by coalescence instability. j_z, z component of the plasma current generating the poloidal magnetic field; λ, scale length of the poloidal magnetic field B_y where the field lines can be considered as straight. λ is small in comparison with the radii of the colliding magnetic ropes R.

the adiabatic constant; λ is the thickness of the current sheet. The plasma is assumed to be sufficiently magnetized allowing for the neglecting of the ion temperature, hence the pressure P_0 is associated with the electron temperature.

Introducing a small parameter $\epsilon = \omega_i^2/\omega_e^2 = m_e/m_i$ and the normalized time $s = t\omega_i$, we rewrite Eqs. (1) and (2) as

$$\frac{d^2 a}{d s^2} = -\frac{1}{\epsilon}\left\{\frac{a}{b} - 1 + \frac{\phi}{a^2} - \frac{\psi}{a^\gamma}\right\}, \qquad (3)$$

$$\frac{d^2 b}{d s^2} = 1 - \frac{b}{a}, \qquad (4)$$

where $\phi = (V_A/\lambda\omega_i)^2$ and $\psi = (V_s/\lambda\omega_i)^2$ are dimensionless constants.

Using the static solution of (3)–(4) obtained for $d/ds = 0$,

$$\bar{a} = \bar{b} = \left(\frac{\phi}{\psi}\right)^{\frac{1}{2-\gamma}} = \left(\frac{V_A^2}{V_s^2}\right)^{\frac{1}{2-\gamma}} = \left(\frac{B_0^2}{4\pi P_0}\right)^{\frac{1}{2-\gamma}}, \quad (5)$$

and normalizing (3)–(4) to the dimensionless value $\bar{a}$, we can rewrite Eqs. (1)–(2) as

$$\frac{d^2 A}{d\tau^2} = -\frac{1}{\epsilon}\left\{\frac{A}{B} - 1 + \frac{\bar{\phi}}{A^2} - \frac{\bar{\phi}}{A^\gamma}\right\}, \qquad (6)$$

$$\frac{d^2 B}{d\tau^2} = 1 - \frac{B}{A}, \qquad (7)$$

with $a(s) = \bar{a} A(\tau)$, $b(s) = \bar{a} B(\tau)$, $s = \bar{a}^{1/2}\tau$, and $\phi = \bar{a}^2 \bar{\phi}$. In this normalization the quantity A is equal to unity at the initial instant of time $A(\tau)|_{\tau=0} = 1$.

A. Nonlinear analysis with the Bernoulli pseudopotential

As ϵ tends to 0, for the left-hand side of Eq. (6) to be finite, the term $\{..\}$ on the right-hand side must tend to zero. This condition in turn allows one to determine the explicit dependence $B(A)$:

$$B(A) = \frac{A^{\gamma+3}}{A^{\gamma+2} - \bar{\phi}(A^\gamma - A^2)}, \qquad (8)$$

which reduces to $A = B$ in the limit considered in [12] for small values of the parameter $\bar{\phi}$. We would like to point out that in the general case when $A \neq B$, considered in

this paper, in addition to the expansion used in (8), another asymptotic expansion of set (6)–(7) is also possible. Namely, introducing the rapid time scale into the problem through the re-normalization of the time variable τ to the small parameter $\sqrt{\epsilon}$ as $\bar{\tau} = \tau/\sqrt{\epsilon}$, the function B demands to be linearly dependent upon $\bar{\tau}$, $B(\bar{\tau}) = C_1\bar{\tau} + C_2$ with C_1 and C_2 being a constants [see Eq. (7)]. The latter group of solutions describes the nonoscillatory behavior of the ion plasma component in the current sheet, accompanied with the higher frequency oscillations of inertialess electrons, and is beyond the scope of the current analysis.

Substituting (8) into (7) results in the second-order ordinary differential equation (ODE) for the function $A(\tau)$:

$$f(A)\frac{d^2 A}{d\tau^2} + \frac{d f(A)}{d A}\left(\frac{d A}{d\tau}\right)^2 = g(A), \qquad (9)$$

where the functions $f(A)$ and $g(A)$ are defined as

$$f(A) = \frac{A^{2(\gamma+2)} - 3\bar{\phi}A^{2(\gamma+1)} + \bar{\phi}(\gamma+1)A^{\gamma+4}}{(A^{\gamma+2} - \bar{\phi}A^\gamma + \bar{\phi}A^2)^2}, \qquad (10)$$

$$g(A) = 1 - \frac{A^{\gamma+2}}{A^{\gamma+2} - \bar{\phi}A^\gamma + \bar{\phi}A^2}. \qquad (11)$$

Equation (9) describes oscillatory evolution of the current sheet. Writing $p(A) = dA/d\tau$ allows us to reduce the second-order ODE (9) to the first-order Bernoulli equation:

$$f(A)\frac{d p(A)}{d A} + \frac{d f(A)}{d A}p(A) = \frac{g(A)}{p(A)}, \qquad (12)$$

with the first integral,

$$\frac{1}{2}\left[f(A)\frac{d A}{d\tau}\right]^2 + U_B(A) = \text{const}, \qquad (13)$$

allowing for the application of the mechanical analogy method. Indeed, considering A and τ as a generalized spatial coordinate and time, respectively, Eq. (13) has the form of the conservation energy law with a generalized potential energy $U_B(A)$, also called the Bernoulli pseudopotential:

$$U_B(A) = -\int_1^A f(A)g(A)\, dA. \qquad (14)$$

Analysis of a second-order ODE with the Bernoulli pseudopotential technique [13] is a recent extension of the Sagdeev potential method used, in particular, in [12]. In contrast to the Sagdeev method, this approach allows one to analyze a broader class of second-order ODEs with a squared first derivative, in particular Eq. (9). We emphasise the importance of the Bernoulli technique and its ability to analyze the corresponding type of ODEs, which is crucial for the solution of the general problem with $A \neq B$ [cf. 12]. In the mechanical analogy given by (13) the function $f^2(A)$ acts as an effective mass, and the oscillating "particle" position is governed by the potential $U_B(A)$. In [12] where the particular case $A = B$ was considered, the mass function is a constant, and the Bernoulli potential reduces to the Sagdeev potential. More details about the Bernoulli pseudopotential technique and examples of its application to analysis of nonlinear ion-acoustic waves and super-nonlinear shear Alfvén waves in multicomponent plasmas can be found in [13–16], and in references therein.

Applications of the Bernoulli pseudopotential method to the analysis of nonlinear fluctuations in self-gravitating quantum plasmas and in two- and three-dimensional graphenelike fluids are shown in [17,18], respectively.

B. Small-amplitude limit

We obtain a solution of Eq. (9) by considering the function $A(\tau)$ to be of a small amplitude and with the initial value of unity: $A(\tau) = 1 + \eta x(\tau)$. In this first-order expansion η is a small parameter, and $x(\tau)$ characterizes the small-amplitude variations of the function $A(\tau)$. Substitution of this expansion to Eqs. (10) and (11) gives, up to the first order of η:

$$f = [1 - \bar{\phi}(2 - \gamma)] + \eta x \bar{\phi}\{6 - \gamma(\gamma + 1) - 2(2 - \gamma)$$
$$\times [1 - \bar{\phi}(2 - \gamma)]\}, \text{ and } g = \eta x \bar{\phi}(2 - \gamma). \quad (15)$$

Using (15) to rewrite Eq. (9), and neglecting the terms higher than the first order of η, we obtain

$$\frac{d^2 x}{d\tau^2} + \frac{\bar{\phi}(2 - \gamma)}{\bar{\phi}(2 - \gamma) - 1} x = 0. \quad (16)$$

Equation (16) is a harmonic oscillator equation with the period,

$$P = 2\pi \left(1 + \frac{1}{\bar{\phi}(\gamma - 2)}\right)^{1/2}, \quad (17)$$

in the normalized units. For $\gamma = 3$, the expression reduces to $P = 2\pi(1 + \bar{\phi}^{-1})^{1/2}$, and tends to 2π for large values of $\bar{\phi}$.

III. NONLINEAR OSCILLATIONS

Consider specific examples of the Bernoulli pseudopotential energy $U_B(A)$ given by Eq. (14) and the corresponding numerical solutions of Eq. (9) for various combinations of the initial parameters. Figure 2 shows that the profile U_B has a minimum at the point $A = 1$, corresponding to the stable equilibrium state of the current sheet, determined by static solution (5). Such a profile allows for the existence of both linear and nonlinear periodic solutions of Eq. (9) above the equilibrium. Two different cases of U_B were found: when its left-hand slope, with respect to the minimum, slope reaches the maximum value faster than the right-hand slope, and the other case when the right-hand slope reaches the maximum faster. The behavior is prescribed by the value of the parameter $\bar{\phi}$. The threshold value of $\bar{\phi}$ which determines when U_B changes the behavior, is about 0.685. At that value of $\bar{\phi}$ the maximum values of the left and right slopes of U_B have the same heights.

Figure 3 shows the time variations of the plasma species concentrations n_e and n_i, obtained numerically from (9), and corresponding to the different cases of U_B shown in Fig. 2. As follows from Eq. (8), the charge separation reaches a large value for large values of $\bar{\phi}$, and is almost negligible for small $\bar{\phi}$. Top panels of Fig. 3 demonstrate two essentially opposite limits: small-amplitude quasilinear oscillations obtained near the bottom of the potential well where it can be approximated by a parabolic function, and large-amplitude nonlinear oscillations obtained near the limit height of $U_B(A)$ (see Fig. 2). The total energy of oscillations of a pseudoparticle in a pseudopotential well is determined by the initial value of the first derivative of a generalized coordinate
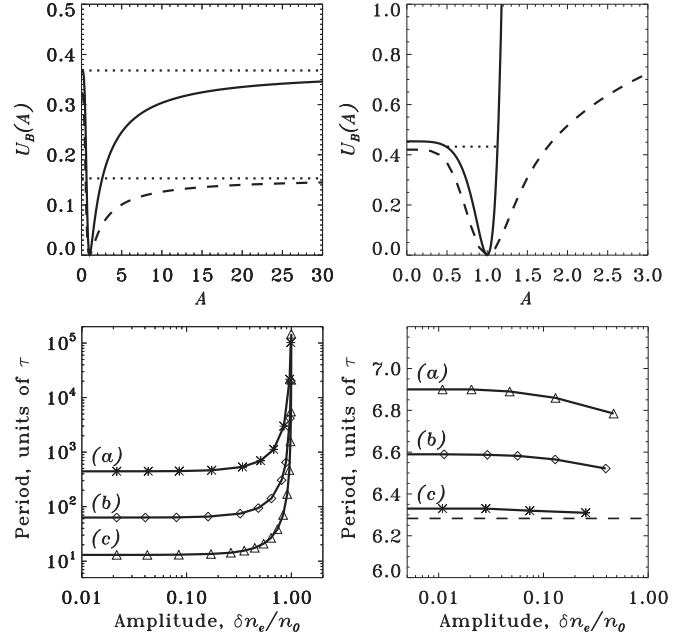

FIG. 2. (Top) Bernoulli pseudopotential $U_B(A)$ (14) plotted for $\gamma = 3$ and for $\bar{\phi} = 0.685$ (left solid), $\bar{\phi} = 0.3$ (left dashed), and $\bar{\phi} = 5$ (right solid), $\bar{\phi} = 2$ (right dashed). The upper horizontal dotted line in the left panel shows the energy level above which $U_B(A)$ experiences the change of behavior; the bottom dashed line shows the energy level of the oscillation shown in Fig. 3, left bottom panel. The horizontal dotted line in the right panel indicates the energy level of the nonlinear signal shown in Fig. 3, right top and bottom panels. (Bottom) The oscillation period-amplitude dependence shown for $\bar{\phi} = 2 \times 10^{-4}$ (a), 10^{-2} (b), and 0.3 (c) (the small $\bar{\phi}$ regime, left panel), and for $\bar{\phi} = 5$ (a), 10 (b), 100 (c) (the large $\bar{\phi}$ regime, right panel), and $\bar{\phi} \to \infty$ (the period equals to 2π, dashed line). The period is measured in units of $(V_s/V_A)^{1/2}\omega_i^{-1}$.

with respect to a generalized time, meaning the kinetic energy of an initial excitation (13). In this study nonzero values of the first derivatives used as the initial conditions for (9) correspond to the speed of the coalescence of the ropes.

According to Eq. (17), for small amplitudes, the oscillation period grows to arbitrarily long values for small $\bar{\phi}$, while for large $\bar{\phi}$ the period tends to the constant value $2\pi(V_s/V_A)^{1/2}\omega_i^{-1}$ in the physical units. The bottom panels in Fig. 2 show the dependence of the period on the amplitude of the electron concentration variations δn_e in the nonlinear regime. For $\bar{\phi} < 0.685$ the period is highly dependent upon the amplitude. For $\bar{\phi} > 0.685$ the oscillations are approximately isochronous (their period depends weakly upon the amplitude even in the nonlinear regime), that can be explained by the shape of the function $U_B(A)$ with the corresponding value of $\bar{\phi} = 5$ (see Fig. 2, top right panel). Indeed, when $\bar{\phi} = 5$, the maximum value of the right slope of U_B is located much above the left one, which results in the almost symmetric shape of U_B in the regions supporting oscillations. Although dependence (17) was initially derived for the small-amplitude linear solutions of Eq. (9), the isochronous nature of the illustrative examples in Figs. 2 and 3 allows one to utilize it for the nonlinear oscillations, too, when large values of $\bar{\phi}$ are considered. For
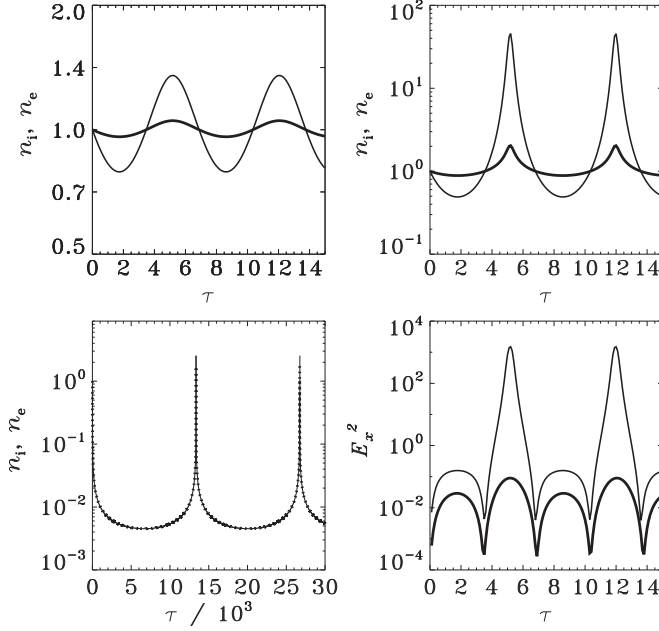
FIG. 3. (Top) Variations of the electron $n_e = n_0/a$ (thick lines) and ion $n_i = n_0/b$ (thin lines) concentrations, where the scale factors a and b are obtained from the numerically obtained solutions $A(\tau)$ of Eq. (9) with $\gamma = 3$, $\bar{\phi} = 5$, $A(0) = 1$, and $\frac{dA}{d\tau}|_{\tau=0} = 0.04$ (left panel, quasilinear oscillation), and $\frac{dA}{d\tau}|_{\tau=0} = 0.155$ (right panel, nonlinear oscillation). (Bottom left) Variations of n_e (dotted line) and n_i (solid line, almost indistinguishable from the dotted line) for $\gamma = 3$, $\bar{\phi} = 0.3$, $A(0) = 1$, and $\frac{dA}{d\tau}|_{\tau=0} = 0.426$ (highly nonlinear case). Both functions n_e and n_i are normalized to $n_0\bar{a}^{-1}$. (Bottom right) Variation of the electrostatic field energy E_x^2 normalized to $(4\pi en_0\lambda\bar{a}^{-1})^2$, generated by the local charge separation, in the quasilinear (thick line) and nonlinear (thin line) regimes of the current sheet oscillation, shown in the top panels. The vertical axes in all panels are plotted on a logarithmic scale. The time τ is measured in units of $(V_s/V_A)^{1/2}\omega_i^{-1}$.

small $\bar{\phi}$ (when $\bar{\phi} < 0.685$, see Fig. 2) the shape of U_B allows for longer-period oscillations.

The electrostatic field $E_x(\tau)$ generated by the local charge separation with the use of Poisson's equation is given by

$$E_x(\tau) = \frac{4\pi en_0\lambda}{\bar{a}}\left(\frac{1}{B(\tau)} - \frac{1}{A(\tau)}\right), \qquad (18)$$

where $A(\tau)$ is obtained numerically from Eq. (9) (see Fig. 3), and $B(\tau)$ from Eq. (8). In Eq. (18) the expressions $n_0/\bar{a}_0 B$ and $n_0/\bar{a}_0 A$ correspond to the ion and electron concentrations, n_i and n_e, respectively.

While the cases for $\bar{\phi} < 0.685$ result in long-period oscillations with small local electric charge separation (see Fig. 3), and hence, give low values of the electric field E_x, larger values of $\bar{\phi}$ allow for short-period oscillations with large electric field; see Fig. 3. A small-amplitude solution of Eq. (9) results in periodic small-amplitude variations of E_x^2, which are still quasiharmonic with a doubled period. In the nonlinear case, the oscillations have large amplitude spikes of the electric field with a clear asymmetry of the positive and negative half-periods. The highest electric field is generated during the positive half-periods of the density oscillations when the strongest charge separation occurs.

IV. DISCUSSION AND CONCLUSIONS

We have found a nonlinear oscillatory regime of the evolution of a current sheet formed by a coalescence of two magnetic flux ropes, which is accompanied by a significant electric charge separation and generation of a strong electric field. The characteristic time scales are shorter than the time of magnetic reconnection that is neglected. Specific regimes of the oscillations are determined by the dimensionless parameter $\bar{\phi} = (V_A/V_s)^6(\lambda_D/\lambda)^2 \approx \beta^{-3}(\lambda_D/\lambda)^2$ (6), where λ is the characteristic thickness of the current sheet, $\lambda_D = V_s/\omega_i$ is the plasma Debye length, and β is the ratio of gas and magnetic pressures in the plasma. These nonlinear oscillations are rather intrinsic, and may occur in coalescence of magnetic islands in natural (e.g., solar, space, magnetospheric) and laboratory plasmas.

The solutions obtained for small values of the parameter $\bar{\phi} < 0.685$ describe perpendicular oscillations of the current sheet, when electrons and ions oscillate almost together and the effects of the local electric charge separation are negligibly small. The $\bar{\phi} = 0$ limit gives the solutions found in [12] for $n_e = n_i$. For sufficiently thin current sheets (i.e., for $\lambda \approx \lambda_D$) this regime is reached when the plasma is of sufficiently high β. For thicker sheets ($\lambda \gg \lambda_D$) this regime can be achieved for smaller β. For $\bar{\phi} > 0.685$, the oscillations produce high spikes of the electric field caused by the electric charge separation. In both regimes, low amplitude oscillations have a harmonic shape, while high amplitude oscillations have a highly anharmonic shape: a series of distinct symmetric spikes.

In the small $\bar{\phi}$ regime, the nonlinear oscillation periods reach values that are several orders of magnitude larger than the ion plasma period (see Fig. 2). For example, for a 1-GHz electron plasma frequency and $V_A \approx 4.8 \times 10^2$ km s^{-1} and $V_s \approx 2.4 \times 10^2$ km s^{-1} giving $V_s/V_A \approx 0.5$, typical for the coronal sites of solar flares [19], the current sheet oscillation periods can reach 1 s or longer. Periods of this order of magnitude are often detected in the solar flare emission, e.g., [10,20], and can appear, e.g., in the gyrosynchrotron emission because of the modulation of the local electron plasma frequency [21]. For lower values of β these periods can be reached for thicker current sheets. In the previous example, if the current sheet thickness is 10^3 km with the plasma Debye length of about 1 cm, the 1-s periods occur for the highly nonlinear large-amplitude oscillations with $\delta n_e \approx n_0$.

In the large $\bar{\phi}$ regime, oscillation periods are shorter than for small $\bar{\phi}$, and approach the value $2\pi(V_s/V_A)^{1/2}\omega_i^{-1}$. Thus, for low values of β, which are also observed in solar coronal plasma structures (e.g., $\beta \approx 0.01$ [22]), for the electron plasma frequencies of about 0.4 GHz, typical periods of current sheet oscillations are a few microseconds.

[1] A. T. Y. Lui, J. Geophys. Res. **101**, 13067 (1996).

[2] K. Shibata and T. Magara, Living Rev. Sol. Phys. **8**, 6 (2011).

[3] B. Kliem, M. Karlický, and A. O. Benz, Astron. Astrophys. **360**, 715 (2000).

[4] V. M. Nakariakov, V. Pilipenko, B. Heilig, P. Jelínek, M. Karlický, D. Y. Klimushkin, D. Y. Kolotkov, D.-H. Lee, G. Nisticò, T. Van Doorsselaere, G. Verth, and I. V. Zimovets, Space Sci. Rev. **200**, 75 (2016).

[5] Z. W. Ma and A. Bhattacharjee, Geophys. Res. Lett. **26**, 3337 (1999).

[6] D. A. Uzdensky, Space Sci. Rev. **160**, 45 (2011).

[7] M. Ono, G. J. Greene, D. Darrow, C. Forest, H. Park, and T. H. Stix, Phys. Rev. Lett. **59**, 2165 (1987).

[8] V. Sergeev, A. Runov, W. Baumjohann, R. Nakamura, T. L. Zhang, M. Volwerk, A. Balogh, H. Rème, J. A. Sauvaud, M. André, and B. Klecker, Geophys. Res. Lett. **30**, 1327 (2003).

[9] M. Bárta, B. Vršnak, and M. Karlický, Astron. Astrophys. **477**, 649 (2008).

[10] V. M. Nakariakov and V. F. Melnikov, Space Sci. Rev. **149**, 119 (2009).

[11] M. Karlický, Res. Astron. Astrophys. **14**, 753 (2014).

[12] T. Tajima, J. Sakai, H. Nakajima, T. Kosugi, F. Brunel, and M. R. Kundu, Astrophys. J. **321**, 1031 (1987).

[13] A. E. Dubinov and M. A. Sazonkin, Sov. J. Expt. Theor. Phys. **111**, 865 (2010).

[14] A. E. Dubinov, D. Y. Kolotkov, and M. A. Sazonkin, Plasma Phys. Rep. **37**, 64 (2011).

[15] A. E. Dubinov, D. Y. Kolotkov, and M. A. Sazonkin, J. Tech. Phys. **57**, 585 (2012).

[16] A. E. Dubinov, D. Y. Kolotkov, and M. A. Sazonkin, Plasma Phys. Rep. **38**, 833 (2012).

[17] M. Akbari-Moghanjoughi, Phys. Plasmas **21**, 082707 (2014).

[18] M. Akbari-Moghanjoughi, J. Appl. Phys. **114**, 073302 (2013).

[19] V. M. Nakariakov, V. F. Melnikov, and V. E. Reznikova, Astron. Astrophys. **412**, L7 (2003).

[20] M. J. Aschwanden, Solar Phys. **111**, 113 (1987).

[21] V. M. Nakariakov and V. F. Melnikov, Astron. Astrophys. **446**, 1151 (2006).

[22] Y. Zhang, J. Zhang, J. Wang, and V. M. Nakariakov, Astron. Astrophys. **581**, A78 (2015).